

NONLINEAR ANALYSIS OF FLUID SATURATED SOIL AND ROCK UNDER COMPLEX HYDROMECHANICAL LOADING ON THE BASE OF POROPLASTIC MODELS

S.A. Le-Zakharov*, B.E. Melnikov, A.S. Semenov

Peter the Great St. Petersburg Polytechnic University,
29 Polytechnicheskaya str., St. Petersburg, 195251, Russia

*e-mail: lezakharov@gmail.com

Abstract. The elastic-plastic model is adopted to simulate the behavior of saturated porous material under mechanical and hydraulic loading. Linear strains are calculated with Biot coupled poroelastic equations. Transition to the plastic state is determined by Mohr-Coulomb or Drucker-Prager criterion in Terzaghi effective stress space. Multisurface theory of plasticity algorithms are used for integration of nonlinear constitutive equations. The results of computations show a good agreement in comparison with available experimental data.

1. Introduction

Inelastic deformation of soils is the main cause of damage of basements of buildings. It leads to abnormal maintenance mode of dams and other structures. Prediction of inelastic deformation, damage and fracturing of soils and rocks is a major point in solving mechanical problems in oil and gas industry, including hydraulic fracturing design. Fluid filtration in porous soils and rocks may influence significantly on strain evolution in many cases. Combined with mechanical loads it may lead to accumulation of irreversible strains and fracturing. Necessity of modeling of such processes requires development of coupled poroelastoplastic models and its implementation using effective numerical integration methods.

2. Elastic-plastic model of saturated porous media

Constitutive equations for reversible strains $\boldsymbol{\varepsilon} - \boldsymbol{\varepsilon}^p$ and reversible porosity change $\phi - \phi^p - \phi_0$ are written in the form of coupled Biot equations [1]:

$$\begin{aligned}\boldsymbol{\sigma} &= ({}^4\mathbf{D} + N\mathbf{b}\mathbf{b}) \cdot (\boldsymbol{\varepsilon} - \boldsymbol{\varepsilon}^p) - \mathbf{b}N(\phi - \phi^p - \phi_0), \\ p &= -N\mathbf{b} \cdot (\boldsymbol{\varepsilon} - \boldsymbol{\varepsilon}^p) + N(\phi - \phi^p - \phi_0),\end{aligned}\quad (1)$$

where $\boldsymbol{\varepsilon}, \boldsymbol{\varepsilon}^p$ are total and plastic strain tensors; ϕ, ϕ^p, ϕ_0 are total, irreversible and initial porosity; $\boldsymbol{\sigma}, p$ are macroscopic stress tensor and pore pressure scalar, ${}^4\mathbf{D}$ is an elastic moduli tensor, \mathbf{b} is a poroelastic Biot coefficient tensor, N is a scalar Biot modulus. Yield criteria for transition to plastic mode is

$$\Phi(\boldsymbol{\sigma}'', \mathbf{q}) = 0, \quad (2)$$

where Φ depends on hardening forces \mathbf{q} and generalized effective Terzaghi stress $\boldsymbol{\sigma}''$:

$$\boldsymbol{\sigma}'' = \boldsymbol{\sigma} + \boldsymbol{\beta} p, \quad (3)$$

where $\boldsymbol{\beta}$ is a material parameter characterizing matrix plastic compressibility, usually taken as unity

tensor as for plastically incompressible matrix [1]. Plastic strain $\boldsymbol{\varepsilon}^p$ evolution is described by the flow rule

$$\dot{\boldsymbol{\varepsilon}}^p = \dot{\lambda} \frac{\partial \Gamma(\boldsymbol{\sigma}'', \mathbf{q})}{\partial \boldsymbol{\sigma}''}, \quad (4)$$

where the plastic potential $\Gamma(\boldsymbol{\sigma}'', \mathbf{q})$ depends on $\boldsymbol{\sigma}''$ and \mathbf{q} ; $\dot{\lambda}$ is a plastic multiplier satisfying Kuhn-Tucker conditions:

$$\Phi \leq 0, \quad \dot{\lambda} \geq 0, \quad \dot{\lambda} \Phi = 0. \quad (5)$$

Evolution of \mathbf{q} in case of multilinear isotropic and kinematic hardening satisfies the equation

$$\dot{\mathbf{q}} = \dot{\lambda} \mathbf{H} \cdot \frac{\partial \Gamma(\boldsymbol{\sigma}'', \mathbf{q})}{\partial \mathbf{q}}, \quad (6)$$

where \mathbf{H} is a material parameter.

Irreversible porosity change is associated with the plastic strain by the law [1]

$$\dot{\phi}^p = \boldsymbol{\beta} \cdot \dot{\boldsymbol{\varepsilon}}^p. \quad (7)$$

Differentiation of equation (2) with using (1), (3)–(7) results to the following equation for the plastic multiplier:

$$\dot{\lambda} = \frac{1}{d} \frac{\partial \Phi}{\partial \boldsymbol{\sigma}''} \cdot [\mathbf{D}_1 \cdot \dot{\boldsymbol{\varepsilon}} + \mathbf{e}_1 \dot{\phi}] \quad (8)$$

and to the equations for $\boldsymbol{\sigma}$ and p rates:

$$\begin{cases} \dot{\boldsymbol{\sigma}} = {}^4\mathbf{D}_t^u \cdot \dot{\boldsymbol{\varepsilon}} - \tilde{\mathbf{e}}_t \dot{\phi} \\ \dot{p} = -\tilde{\mathbf{e}}_t \cdot \dot{\boldsymbol{\varepsilon}} + N_t \dot{\phi} \end{cases} \quad (9)$$

where

$$\begin{aligned} {}^4\mathbf{D}_t^u &= {}^4\mathbf{D}^u - \frac{1}{d} \mathbf{D}_1^T \cdot \frac{\partial \Gamma}{\partial \boldsymbol{\sigma}''} \frac{\partial \Phi}{\partial \boldsymbol{\sigma}''} \cdot \mathbf{D}_1, \quad N_t = N - \frac{1}{d} \mathbf{e}_1 \cdot \frac{\partial \Gamma}{\partial \boldsymbol{\sigma}''} \frac{\partial \Phi}{\partial \boldsymbol{\sigma}''} \cdot \mathbf{e}_1, \\ \tilde{\mathbf{e}}_t &= \mathbf{e} + \frac{1}{d} \mathbf{D}_1^T \cdot \frac{\partial \Gamma}{\partial \boldsymbol{\sigma}''} \frac{\partial \Phi}{\partial \boldsymbol{\sigma}''} \cdot \mathbf{e}_1, \quad \tilde{\mathbf{e}}_t = \mathbf{e} + \frac{1}{d} \mathbf{e}_1 \cdot \frac{\partial \Gamma}{\partial \boldsymbol{\sigma}''} \frac{\partial \Phi}{\partial \boldsymbol{\sigma}''} \cdot \mathbf{D}_1, \\ \mathbf{D}_1 &= \mathbf{D}^u - \boldsymbol{\beta} \mathbf{e}, \quad {}^4\mathbf{D}^u = {}^4\mathbf{D} + N \mathbf{b} \mathbf{b}, \quad \mathbf{e}_1 = N \boldsymbol{\beta} - \mathbf{e}, \quad \mathbf{e} = N \mathbf{b}, \\ d &= \frac{\partial \Phi}{\partial \boldsymbol{\sigma}''} \cdot [\mathbf{D}_1 + \mathbf{e}_1 \boldsymbol{\beta}] \cdot \frac{\partial \Gamma}{\partial \boldsymbol{\sigma}''} - \frac{\partial \Phi}{\partial \mathbf{q}} \cdot \mathbf{H} \cdot \frac{\partial \Gamma}{\partial \mathbf{q}}. \end{aligned} \quad (10)$$

Choice of potentials Γ and Φ finally determines the elastic-plastic model of the material.

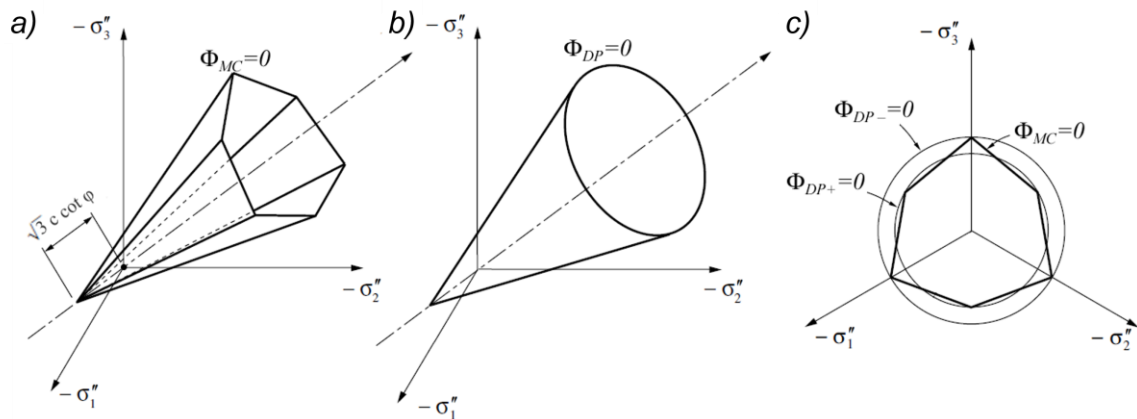


Fig. 1. Yield criteria in Terzaghi principal stress space:

- a) Mohr-Coulomb (MC) yield surface, b) Drucker-Prager (DP) yield surface, c) Comparison of MC and two variants of DP surface [2].

Thus, Mohr-Coulomb (Fig. 1) potential adopted for porous material is written as [3, 4, 5]

$$\Phi = \left(\cos \theta'' - \frac{1}{\sqrt{3}} \sin \theta'' \sin \varphi \right) \sqrt{J_2''} + I_1'' \sin \varphi - c \cos \varphi, \quad (11)$$

where I_1'', J_2'' are appropriate invariants of σ'' and its deviator s'' , φ – internal friction angle (material parameter), c – cohesion (material parameter), θ'' is Lode angle in effective stress space. If Lode angle in (10) is replaced by certain (constant) angle, it leads to the equation for Drucker-Prager potential (Fig. 1). Usually this certain angle is chosen in the way to fit Coulomb-Mohr model in uniaxial tension (“+”) or uniaxial compression (“−”):

$$\Phi = \frac{1}{2\sqrt{3}} (3 \pm \sin \varphi) \sqrt{J_2''} + I_1'' \sin \varphi - c \cos \varphi. \quad (12)$$

3. Model testing and results

Algorithms for numerical integration of constitutive equations (8) based on multisurface plasticity concepts [3] are implemented. Numerical tests for limestone (Fig. 2) and concrete (Fig. 3) under various loading are performed. Calculation results demonstrate a good agreement with experimental data [4-6] under low confining pressures. Laboratory experiment from [6] is also modelled. It illustrates equivalence between mechanical confining compression (tension) and porous pressure decreasing (increasing), that confirms relevancy of choosing Terzaghi stress as a dissipative force.

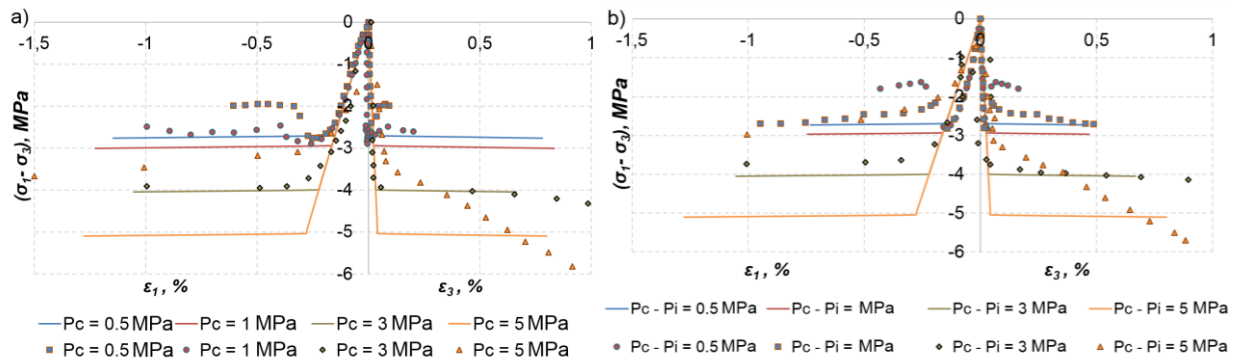


Fig. 2. Triaxial drained compression of limestone (soft loading with drainage). Confining pressure P_c : 0.5, 1, 3, 5 MPa. Pore pressure a) atmospheric ($P_i = 0$), b) $P_i = 2$ MPa. Calculation with Mohr-Coulomb model without hardening. Experiment [4].

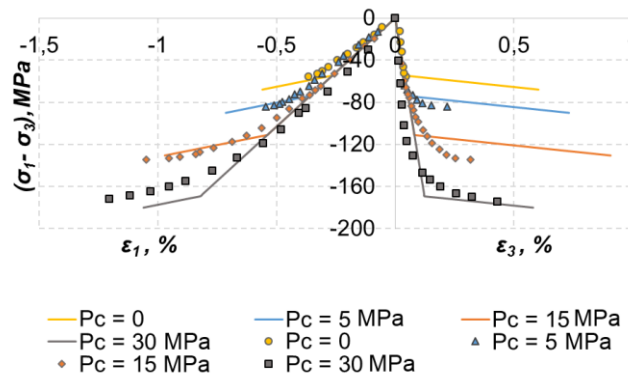


Fig. 3. Triaxial drained compression of concrete (soft loading with drainage). Confining pressure P_c : 0, 5, 15, 30 MPa. Pore pressure $P_i = 0$. Calculation with Mohr-Coulomb model with linear isotropic hardening. Experiment from [5].

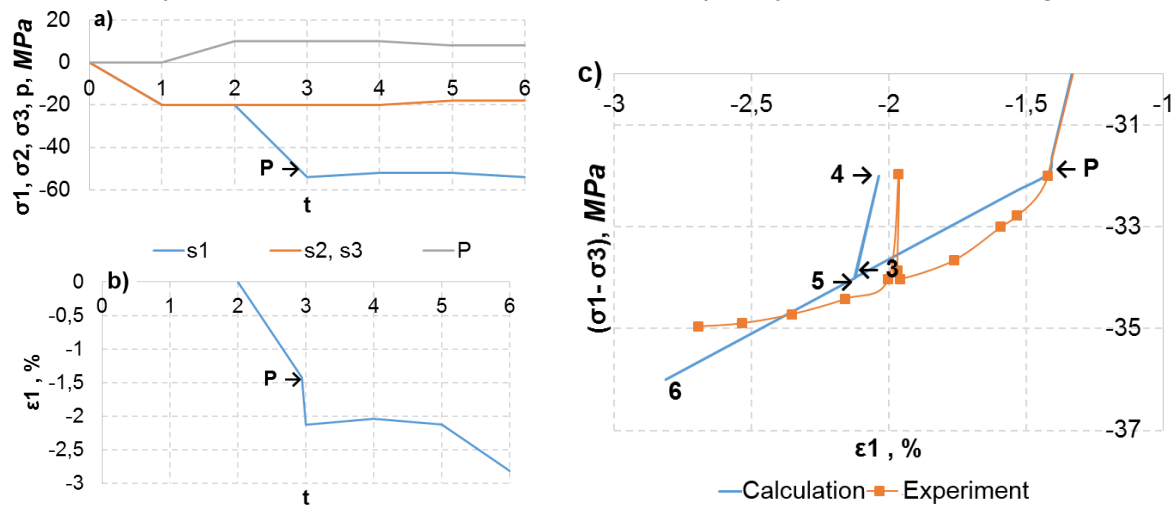


Fig. 4. Illustration of equivalence of confining mechanical compression and decreasing of pore pressure in limestone under combined loading: a) loading history; b) strain ε_1 evolution; c) load curve $\varepsilon_1(\sigma_1 - \sigma_3)$. Section 0-1: triaxial compression up to 20 MPa; 1-2: pore pressure increasing up to 10 MPa; 2-3: triaxial compression with uniaxial prevalence (up to 54 MPa); “P” – yield point; 3-4: unloading (down to 52 MPa); 4-5: restoring of σ'' due to confining pressure decreasing from 20 down to 18 MPa and pore pressure decreasing down to 8 MPa; 5-6: further loading with plastic strains development. Experiment [6].

Acknowledgements. The work was carried out supported by the grant of Russian Fund for Fundamental Research No 16-29-15121.

References

- [1] O. Coussy, *Poromechanics* (Wiley, UK, 2004).
- [2] E.A. de Souza Neto, D. Peric, D.R.J. Owen, *Computational methods for plasticity. Theory and applications* (Wiley, UK, 2008).
- [3] I.N. Izotov, N.P. Kuznetsov, B.E. Melnikov, A.G. Mityukov, A.Y. Musienko, A.S. Semenov // *Proceedings of SPIE* **4348** (2001) 390.
- [4] S.Y. Xie, J.F. Shao // *Rock Mechanics and Rock Engineering* **48**(1) (2015) 223.
- [5] H. Yang, Y. Jia, S.Y. Xie, J.F. Shao // *Transport in Porous Media* **102** (2014) 427.
- [6] R. Kerbouche, J.F. Shao, F. Skozylas, J.P. Henry // *European Journal of Mechanics-A Solids* **14** (1995) 3577.